



## Technical note

Performance in real condition of photonic crystal sensor based NO<sub>2</sub> gas monitoring system

M. Rahmat<sup>a,b,\*</sup>, W. Maulina<sup>b</sup>, E. Rustami<sup>b</sup>, M. Azis<sup>b</sup>, D.R. Budiarti<sup>b</sup>, K.B. Seminar<sup>a</sup>,  
A.S. Yuwono<sup>c</sup>, H. Alatas<sup>b,\*\*</sup>

<sup>a</sup> Department of Mechanical and Biosystem Engineering, Faculty of Agriculture Engineering and Technology, Bogor Agricultural University, Kampus IPB Darmaga, Bogor, West Java 16680, Indonesia

<sup>b</sup> Department of Physics, Faculty of Mathematics and Natural Sciences, Bogor Agricultural University, Kampus IPB Darmaga, Bogor, West Java 16680, Indonesia

<sup>c</sup> Department of Civil and Environmental Engineering, Faculty of Agriculture Engineering and Technology, Bogor Agricultural University, Kampus IPB Darmaga, Bogor, West Java 16680, Indonesia

## ARTICLE INFO

## Article history:

Received 9 March 2013

Received in revised form

17 May 2013

Accepted 22 May 2013

## Keywords:

Photonic crystal

NO<sub>2</sub> gas

Real-time monitoring system

## ABSTRACT

In this report we discuss the performance in real condition of an optical based real-time NO<sub>2</sub> gas monitoring system. For detecting the gas concentration in the ambient air we have developed an optical sensor based on one-dimensional photonic crystal with two defects that allows the existence of photonic pass band inside the associated photonic band gap. To measure the gas concentration, we dissolve the corresponding NO<sub>2</sub> gas into a specific Griess Saltzman reagent solution. The change of gas concentration in the related dissolved-solution can be inspected by the photonic pass band peak variation. It is observed that the wavelength of the photonic pass band peak of the fabricated photonic crystal is nearly coincide with the wavelength of the associated solution highest absorbance. The laboratory test shows that the device works properly, whereas the field measurement test demonstrates accurate results with validation error of 1.56%.

© 2013 Elsevier Ltd. All rights reserved.

## 1. Introduction

NO<sub>2</sub> gas is one of the NO<sub>x</sub> gas types that should get more attention due to its effect to human (Brunekreef, 2007). Its impact to health depends on the concentration, exposure time and individual susceptibility. Long exposure time and high concentration will lead to the reduction of lung function, respiratory disorders and asthma (Gauderman et al., 2005). The transportation sector contributes the highest emission in Asia and America besides the power generators and industries (USEPA, 2006). Obviously, detection and measurement of NO<sub>2</sub> gas should be of our concern.

Semiconductor or optical platforms are commonly used in the gas sensor devices. The semiconductor based sensor has been

developed by many researchers, either in the form of thin film (Meixner et al., 1995) or nanowire (Zhang et al., 2004). Meanwhile, the optical based sensor has also been developed rapidly in recent years. A periodic optical system called photonic crystal (PhC) has been widely used in a refractive index sensing system (Koronov and Zheltikov, 2005) due to the existence of photonic band-gap (PBG). Inside PBG no light can propagate.

Recently, a refractive index sensor based on one dimensional PhC with two defects has been proposed (Alatas et al., 2006). This PhC consists of two dielectric materials in a unit cell with different refractive indices which are arranged in alternating stack on one direction. These two defects create a photonic pass-band (PPB) inside the corresponding PBG. In this narrow band light can propagate. It was demonstrated that by changing the optical path of the first defect that close to the light source, the PPB position is shifted. Meanwhile, because resonance field in the second defect occurred due to leakage-cavity-mode from the first defect (Alatas et al., 2006), its optical path variation leads to the change of PPB peak while its position is unshifted. This phenomenon has been used for refractive index sensing of liquid (Rahmat et al., 2009).

\* Corresponding author. Department of Physics, Faculty of Mathematics and Natural Sciences, Bogor Agricultural University, Kampus IPB Darmaga, Bogor, West Java 16680, Indonesia.

\*\* Corresponding author.

E-mail addresses: [m.rahmat@ipb.ac.id](mailto:m.rahmat@ipb.ac.id) (M. Rahmat), [alatas@ipb.ac.id](mailto:alatas@ipb.ac.id) (H. Alatas).

In this report we discuss the performance in real condition of a sensor device based on one dimensional PhC with two defects for monitoring the concentration of NO<sub>2</sub> gas. The gas is dissolved in a specific reagent to take into account the Beer Lambert effect.

## 2. Materials and method

### 2.1. Fabrication of one dimensional photonic crystals with two defects and its characterization

As illustrated in Fig. 1, we consider a PhC structure with three regular grating segments assigned by N, L and M-segment with number of cells in each of them is 4, 6 and 2, respectively. We inserted the two defect cells between N-L and L-M segments, such that there are 28 stacked layers in this configuration including the defects. The regular unit cell in each segments consist of two dielectric materials namely OS-5 (alloy of ZrO<sub>2</sub> and TiO<sub>2</sub>) and MgF<sub>2</sub> with refractive indices of 2.1 and 1.38 and layer thickness of 66 nm and 100 nm, respectively. The OS-5 layer in the first defect cell is set to different thickness namely 132 nm, while a layer in the second defect cell is set as a receptor to be filled by an analyte. In both defects the thickness of MgF<sub>2</sub> layer is similar to regular cell. Here, we used the variation of PPB peak with respect to the change of analyte as a sensing signature, where its fixed position allows us to use a low cost photo detector. This is in contrast with previous sensing mechanism that use the shifting of PPB peak as its signature (Sünner et al., 2008; Feng et al., 2012). The transfer matrix method based simulation (Alatas et al., 2006) of PPB variation with respect to the change of analyte along with its Q-factor ( $\lambda_{\text{peak}}/\Delta\lambda_{\text{FWHM}}$ ) is given in Fig. 2 where the corresponding PPB peak position is at 550 nm. As expected, it shown that the Q-factor is proportional to the change of analyte refractive index, which indicates that the decreasing of PPB peak is due to the increasing of confined field in the second defect layer.

The PhC was fabricated using electron beam evaporation device (Maulina et al., 2011). In the process, we prepared two flat substrates (denoted by substrate-1 and substrate-2) made from borosilicate crown glass or BK-7 with refractive index of 1.52. This glass is transparent in the wavelength range of 300–2000 nm. In the vacuum chamber we grew on top of the substrates the OS-5 and MgF<sub>2</sub> materials alternately with configuration shown in Fig. 1. The vacuum pressure is set to 10<sup>-3</sup> Pa at temperature of 573 K. The coating process is done in the following steps: (i) coat the first 8 layers or 4 unit cells on the BK-7 substrate-1 (ii) create the first defect layer (iii) add the next 13 layers on top of the first defect (iv) create the 28 to 24-th layer also on a BK-7 substrate-2 (v) leave the 23-th layer to be filled by analyte.

After fabrication, we checked its transmittance characteristic using Olympus USPM spectrophotometer. We also measured the absorbance wavelength of NO<sub>2</sub> dissolved reagent solution. For this,

we prepared the solution sample by injecting the gas, which is extracted from ambient air using vacuum pump, into the GS reagent and characterizes its wavelength absorbance using UV–VIS spectrophotometer Ocean Optics USB 2000. We put the solution into a cuvette in a sample holder and illuminate it with a LS-1 tungsten halogen lamp. The experimental scheme to characterize the PhC with empty receptor is illustrated in Fig. 3a. As shown in Fig. 4, it was found that the PPB peak position of the fabricated PhC and the highest absorbance of NO<sub>2</sub> gas is nearly coincide.

The maximum absorbance wavelength is observed at the range of 500–600 nm, with the highest peak is found at 550 nm. In the meantime, the PPB peak position of the fabricated PhC is found at 533.16 nm as shown in Fig. 4. The difference between actual peak position from the simulation result (550 nm) is due to the unavoidable device precision during the fabrication process. Nevertheless, this value is still within the range of maximum absorbance of the NO<sub>2</sub> dissolved solution (See Fig. 4).

### 2.2. Sensor device

Illustrated in Fig. 3b is the sensor device consisting of a PhC sensor, an impinger, a light source and a photo detector which is connected to an electronic instrumentation system and consists of an analog signal conditioning (ASC) and a microcontroller system.

As seen in Fig. 4, the absorbance spectrum of NO<sub>2</sub> dissolved reagent solution is in the wavelength region of 500–600 nm and the fabricated PhC has PPB peak wavelength at 533.16 nm. Based on this, we choose a photodiode made by Optronic EPIGAP with operational wavelength between 490 and 560 nm. As a light source, we use a commercial LED with wavelength around 530 nm.

In ASC system, for the current to voltage converter we choose the trans-impedance amplifier (TIA) circuit system based on LMC660 IC from National Semiconductor. This component is selected based on the small value of input bias current (~2 fA). The TIA circuit stability is affected by the photodiode characteristics. One of the potential aspects to bring noise to the DC voltage output is the source capacitor ( $C_s$ ), an intrinsic characteristic of the photodiode. To compensate it, we consider the combination of an external feedback capacitor ( $C_f$ ) and a resistor ( $R_f$ ). Using Orcad Capture PSpice 9.2 Professional software it was found that the effect of noise due to  $C_s$  can be reduced by parallel combination of both  $C_f$  and  $R_f$ . It is important to be noted that the related noise cannot be completely removed.

The other parts of ASC system are the voltage amplifier and analog low pass filter circuits. The PGA Burr-Brown 204 amplifier is used to enhance the voltage signal up to 1000 times. Unfortunately, this signal enhancement also enlarges the previous noise from TIA system. To reduce this noise, we added a passive analog low pass filter circuit with a cut-off frequency of 1 Hz.

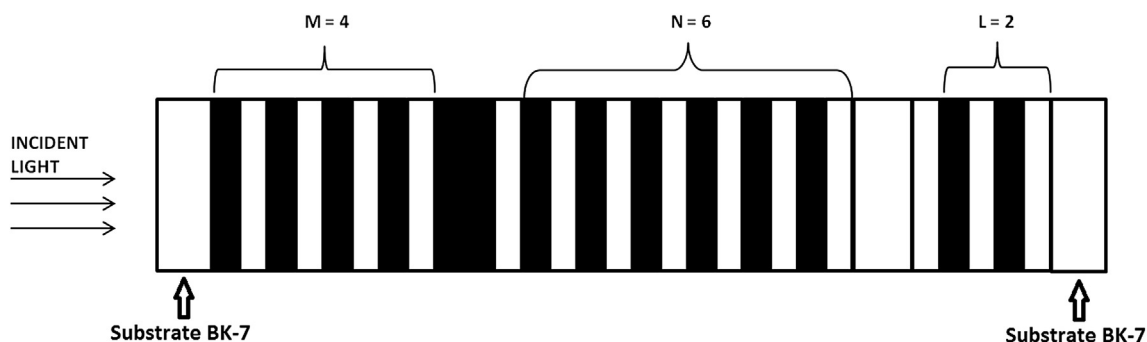


Fig. 1. Design of photonic crystal structure.

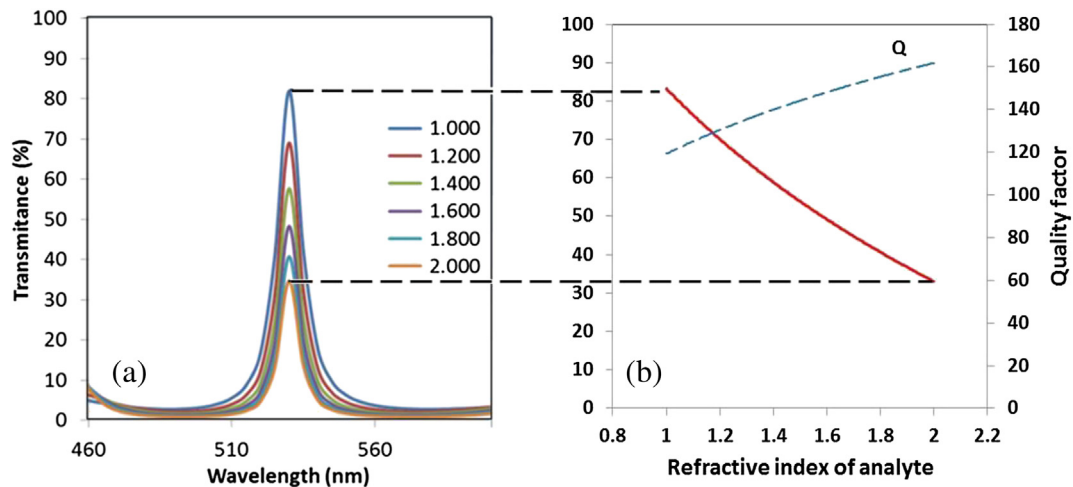


Fig. 2. Simulation result of photonic crystal (a) PPB transmittance spectra 4-6-2 PhC model. (b) Correlation between PPB peak and refractive index in second defect layer (red solid curve) and the corresponding Q-factor (blue dash curve). (For interpretation of the references to color in this figure legend, the reader is referred to the web version of this article.)

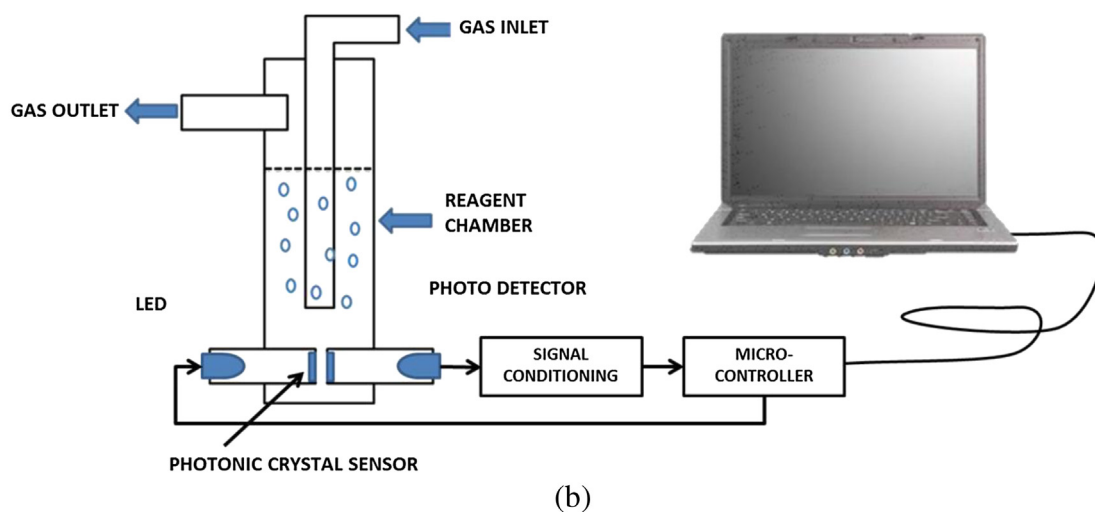
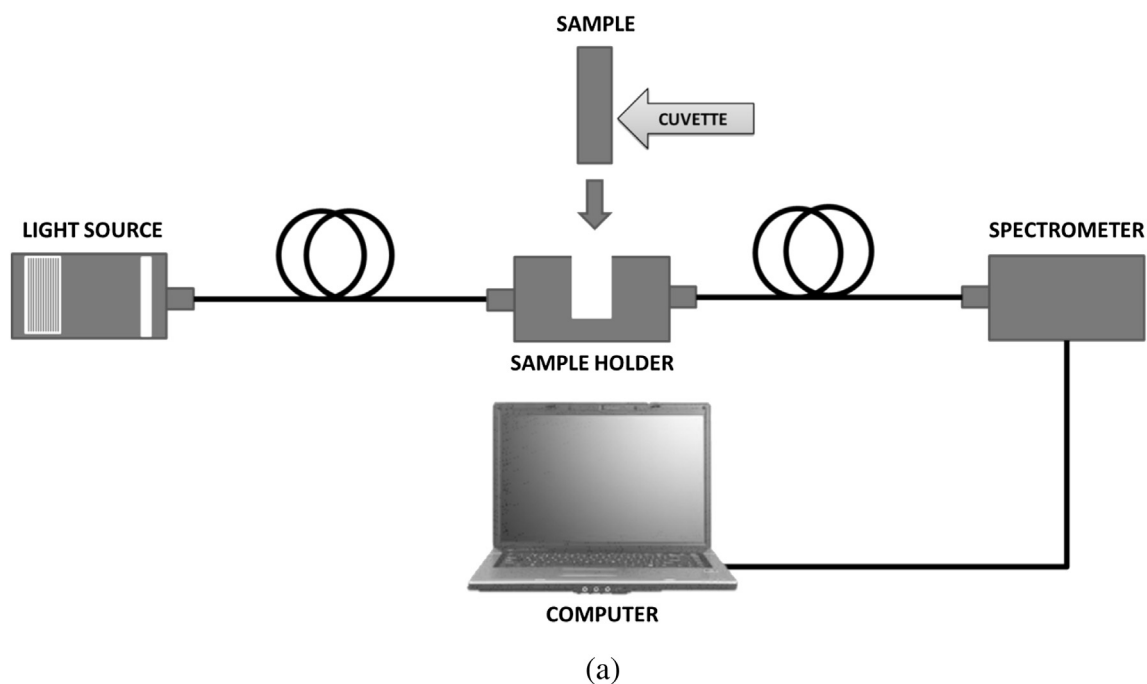


Fig. 3. Schematic diagram (a) experimental setup (b) PhC sensor device. (For interpretation of the references to color in this figure legend, the reader is referred to the web version of this article.)

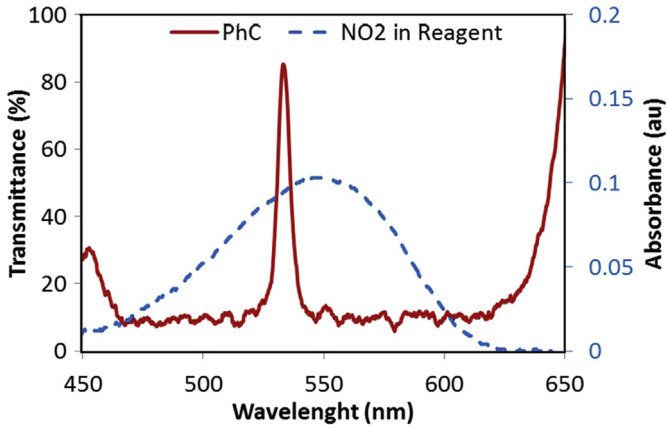


Fig. 4. Comparison of optical characteristics between PhC (red solid line) and NO<sub>2</sub> gas in reagent solution (blue dash line). (For interpretation of the references to color in this figure legend, the reader is referred to the web version of this article.)

For microcontroller system, we use a DFRduino Mega 1280 from DFRobot. The analog voltage output from the ASC system is further converted into digital voltage by the internal analog to digital converter (ADC) of microcontroller. We set the microcontroller to collect data from ASC system in every two minutes such that there are 31 data collected for a single capture. To get a representative single output from the data we use the median filter method namely by sorting them and find its middle value (median). The median filter method with insertion algorithm for data sortation shows faster processing time and more robust against outlier data.

### 3. Results and discussion

Prior to field measurements, the device was laboratory tested to examine its response performance with respect to the change of NO<sub>2</sub> concentration absorbed in the reagent solution. The testing is carried out in three steps using the configuration given in Fig. 3b as follows: (i) Disconnect the ASC and microcontroller from the sensor device and use spectrophotometer as photo detector to examine

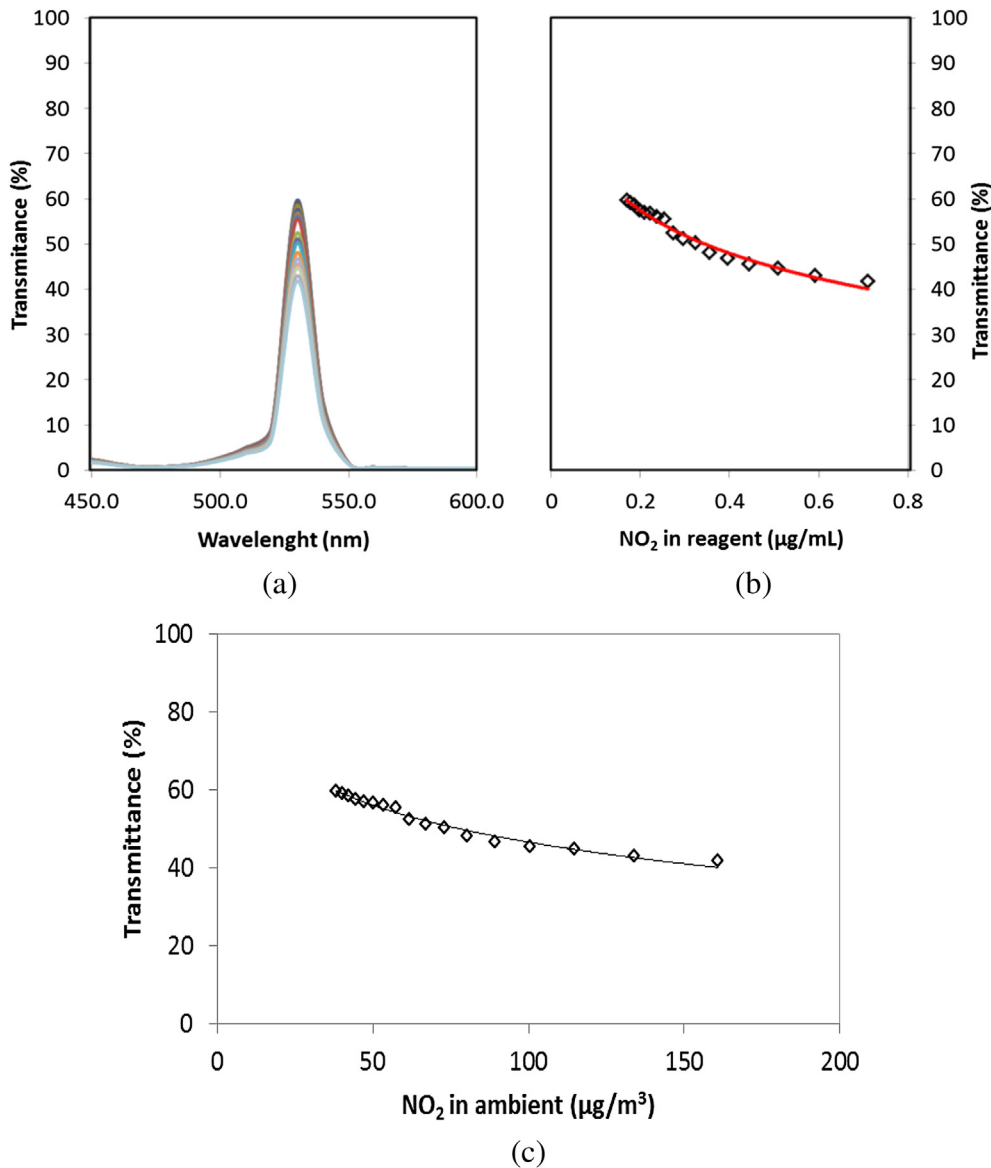
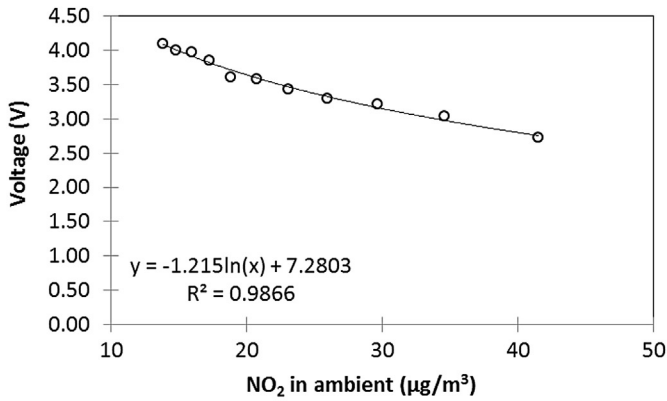
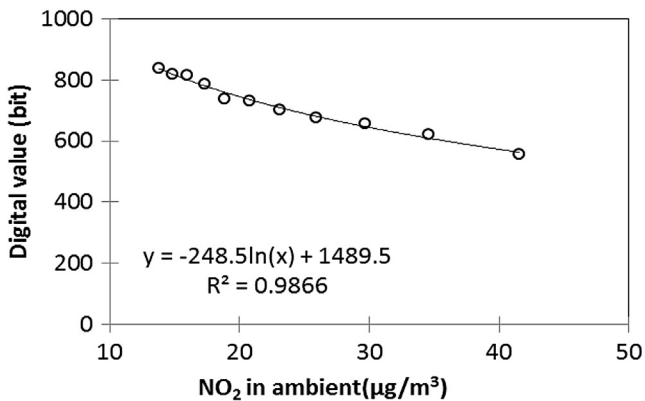


Fig. 5. Experiment result (a) PPB spectra in variation of concentration of NO<sub>2</sub> in reagent solution (b) correlation between PPB peak transmittance and concentration of NO<sub>2</sub> in reagent solution (c) the correlation between PPB transmittance NO<sub>2</sub> concentration in ambient air. (For interpretation of the references to color in this figure legend, the reader is referred to the web version of this article.)



(a)



(b)

Fig. 6. The correlation between the concentration of NO<sub>2</sub> with an intensity that has been converted into (a) units of voltage (V) (b) digital values in bit unit.

the spectral characteristics of the device around the PPB, (ii) replace the spectrophotometer with a photodiode and reconnect the ASC to the sensor and to examine its response with respect to the change of gas concentration we use digital multimeter as well as oscilloscope to study the ASC output noise characteristics, (iii) perform the test of microcontroller output in bit units. Note that to meet the required condition for the Beer Lambert effect measurement, all these tests were conducted under the same cross sectional area and thickness of receptor, while the gas concentration was varied.

In the first step, the conducted experiment gives the relation between the spectral variations of PPB with respect to the change of NO<sub>2</sub> concentration in the reagent solution as shown in Fig. 5a. The PPB peak as a function of NO<sub>2</sub> weight per unit volume of reagent, shows a monotonous relation with negative gradient. For more representative information, we transform the data of PPB peak as a function NO<sub>2</sub> gas weight per unit ambient air volume as follows: the collected data is found from 1 h experiment where the flow rate of air inhaled through the reagent solution into the impinger is about 0.4 l min<sup>-1</sup>. The average inhaled air volume is 22.63 l. Here, we use 10 ml GS reagent and from the obtained concentration of NO<sub>2</sub> in the reagent as given in Fig. 5b, we can calculate the concentration of NO<sub>2</sub> in ambient air and the result is given in Fig. 5c. It was found that the increase of NO<sub>2</sub> concentrations leads to the decreasing of PPB peak which can be approximated by a logarithmic function with a regression coefficient of R<sup>2</sup> = 0.9779. The results of this experiment are in agreement with numerical simulations of PPB peak as a function of defect layer refractive index (Fig. 2). By comparing visually Figs. 2 and 5c, we can predict that the index change of the related reagent solution is between 1.2 and 1.8.

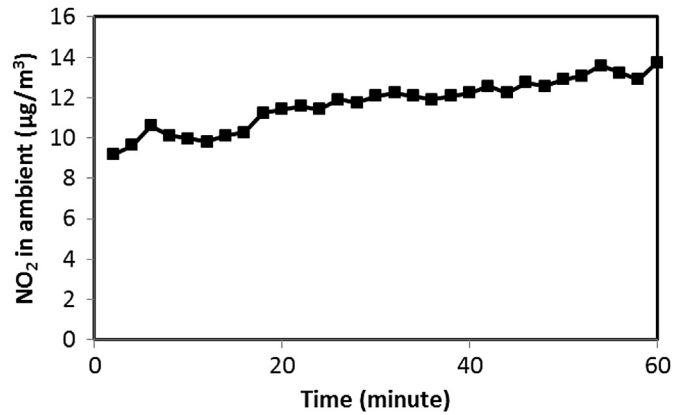


Fig. 7. Concentrations of NO<sub>2</sub> measurement for two minutes interval in real time mode.

We reconnect the ASC to PhC sensor in the second step and use a photodiode as a photo detector to convert light into electric voltage. We use a 530 nm LED as the light source which is illuminated perpendicularly to the PhC sensor system. We measure the device response similar to the previous step but the output is now represented by voltage unit. The purpose of this test is to determine the correlation of NO<sub>2</sub> concentration changes with respect to the light intensity received by the photodiode using a digital multimeter. The relation between the concentration of NO<sub>2</sub> gas in ambient air and the intensity represented in Volt unit, is shown in Fig. 6a, which is consistent with the results of previous step.

In the third step, the data processing is provided digitally via the internal 10-bit ADC of DFRduino ATmega 1280 microcontroller. The voltage value of 0–5 V is converted into a digital value between 0 and 1023 bit and recorded in a computer through a serial port. The correlation between the concentrations of NO<sub>2</sub> and digital values are plotted on the curve in Fig. 6b which can be approximated by a logarithmic function with R<sup>2</sup>=0.9866. Clearly, a consistent output trend which is similar to the previous two steps was found.

In addition, we have examined the measurement with and without PhC separately. The result is given in Fig. 8, showing transmittance as function of logarithmic concentration. The

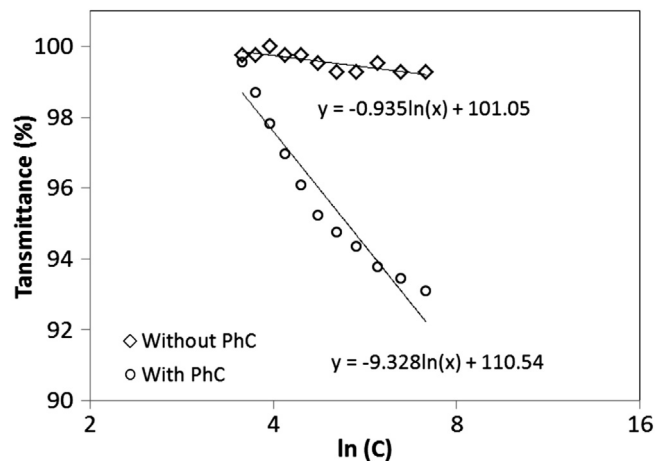


Fig. 8. Comparison of correlation curve of NO<sub>2</sub> concentration between measurements using PhC and without PhC.



gradient for both cases are found to be  $-9.328$  and  $-0.935$ , respectively, which indicates that the presence of PhC play a very significant role.

Next, we perform the in-situ and real time field measurement. The air sampling is conducted in the ambient air in front of the main gate of our campus, which is located at  $65.63^\circ$  S,  $106.725^\circ$  E. The sampling is done by sucking the air into the impinger using a vacuum pump with rate of  $0.4 \text{ l min}^{-1}$ . Measurement data is automatically recorded on a computer every two minutes as well as the temperature and humidity ranges. To predict the gas concentration in ambient air directly in real time mode we program the microcontroller by inserting the logarithmic function found from plotted data in Fig. 6b. The concentration data can be recorded in the specified time period. For example, Fig. 7 shows the measurement results which was carried out in every 2 min.

The accuracy of field measurement is validated using the conventional chemical Griess Saltzman (GS) method which is a standard procedure adopted by the National Standardization of Indonesia (SNI No. 19-7119.2-2005) to test the level of  $\text{NO}_2$  (BSN, 2005). The validation value is obtained by calculating the mean absolute percentage error (MAPE) between the actual data from the field measurement and the validated data from GS method.

In the following we briefly explain the method of GS adopted in SNI. Chemically, it is known that the GS reagent consists of solutions of sulfanilic acid, glacial acetic acid, N-(1-naphthyl)-ethylenediamine dihydrochloride (NEDA), acetone, and free-nitrite-distilled-water. The chemical reaction between  $\text{NO}_2$  molecules and this reagent form a compound of azo dye with pink color which is stable after 15 min.

The gas concentration is further examined by measuring the transmittance of the azo dye at its maximum absorbance wavelength 550 nm. To determine the concentration of  $\text{NO}_2$  gas from the air sample, we calibrate the result by comparing it to another controlled azo dye compound from GS reagent and  $\text{NaNO}_2$  prepared separately. This compound is used as a reference. We prepare a 10 ml GS for the air sample measurement and a 25 ml GS +  $\text{NaNO}_2$  compound for calibration.

To calculate the  $\text{NO}_2$  concentration in the ambient air we use the following formula:

$$C(\mu\text{g m}^{-3}) = \frac{46}{69} \times \frac{10}{25} \times \frac{A}{f} \times \frac{1}{F\Delta t} \times \frac{T_a}{P_a} \times 10^5 \quad (1)$$

Here, the parameter  $A$  denotes the total weight of  $\text{NaNO}_2$ , 46 and 69 are the  $\text{NO}_2$  and  $\text{NaNO}_2$  molecule weight numbers, respectively. The parameter  $f$  represents the mol fraction of  $\text{NaNO}_2$  that produces an equivalent pink color compared to 1 mol  $\text{NO}_2$  and empirically its value is  $f = 0.82$ . The parameter  $F$  is the average flow rate,  $\Delta t$  is the measurement time, and  $P_a$  and  $T_a$  are the average of relative pressure and temperature of ambient air normalized to 760 mmHg and room temperature 298 K, respectively. The conversion factor is given by  $10^5$ . Detailed formulation can be found in ref. (BSN, 2005)

The actual field measurement using the sensor device was performed for an hour in ten days. The results shall be compared with those obtained by the conventional SNI method. The average actual data, denoted by  $\bar{C}_a$ , is subtracted by a validator data, denoted by  $C_v$ , from the GS method, showing the measurement deviation. We define the measurement error as the absolute value of the deviation in measurement  $|C_v - \bar{C}_a|$  divided by  $C_v$ . The average value of the measurement errors is called Mean Absolute Percentage Error (MAPE). The validation data are shown in Table 1 where the MAPE value is 1.56%.

**Table 1**

Validation of  $\text{NO}_2$  gas concentration measurement using PhC sensor device by GS method.

| No   | $C_v(\mu\text{g m}^{-3})$ | $\bar{C}_a(\mu\text{g m}^{-3})$ | $ C_v - \bar{C}_a $ | $ C_v - \bar{C}_a /C_v(\%)$ |
|------|---------------------------|---------------------------------|---------------------|-----------------------------|
| 1    | 135.73                    | 134.01                          | 1.72                | 1.27%                       |
| 2    | 116.65                    | 114.87                          | 1.78                | 1.53%                       |
| 3    | 101.78                    | 100.51                          | 1.28                | 1.26%                       |
| 4    | 91.10                     | 89.34                           | 1.76                | 1.93%                       |
| 5    | 81.34                     | 80.41                           | 0.94                | 1.15%                       |
| 6    | 73.89                     | 73.10                           | 0.79                | 1.07%                       |
| 7    | 68.31                     | 67.01                           | 1.31                | 1.91%                       |
| 8    | 63.20                     | 61.85                           | 1.35                | 2.14%                       |
| 9    | 58.56                     | 57.43                           | 1.13                | 1.92%                       |
| 10   | 54.38                     | 53.61                           | 0.78                | 1.44%                       |
| MAPE |                           |                                 |                     | 1.56%                       |

#### 4. Conclusion

We have discussed the performance of a photonic crystal based integrated sensor for real time and in-situ  $\text{NO}_2$  gas monitoring system. The basic physical mechanism behind this device is the combination of photonic pass band variation phenomenon of photonic crystal with defects and Beer Lambert effect. It is shown that this system can be considered as an alternative platform for monitoring the level  $\text{NO}_2$  concentration in the ambient air. By comparing with the standard chemical based measurement method, it is demonstrated that the results of field measurement using the device are accurate with relatively small MAPE value of 1.56%.

#### Acknowledgment

This research is supported by “Program Beasiswa Unggulan Terpadu” from Ministry of Education and Culture, Republic of Indonesia, under contract no. 70811/A2.5/LN/2010. We thank the Centre for Environmental Research-IPB (PPLH-IPB) that allowed us to use their facilities.

#### References

- Alatas, H., Mayditia, H., Hardhienata, H., Iskandar, A.A., Tjia, M.O., 2006. Single frequency refractive index sensor based on finite one-dimensional photonic crystal with two defects. *Japanese Journal of Applied Physics* 45, 6754–6758.
- Brunekreef, B., 2007. Health effects of air pollution observed in cohort studies in Europe. *Journal of Exposure Science and Environmental Epidemiology* B, S61–S65.
- [BSN] Badan Standardisasi Nasional, 2005. Cara uji kadar  $\text{NO}_2$  dengan metode Griess-Saltzman menggunakan spektrofotometer. SNI No. 19–7119.2-2005.
- Feng, C., Feng, G.Y., Zhou, G.R., Chen, N.J., Zhou, S.H., 2012. Design of an ultracompact optical gas sensor based on a photonic crystal nanobeam cavity. *Laser Physics Letters* 9, 875–878.
- Gauderman, W.J., Avol, E., Lurmann, F., Kuenzli, N., Gilliland, F., Peters, J., McConnell, R., 2005. Childhood asthma and exposure to traffic and nitrogen dioxide. *Epidmiology* 16, 737–743.
- Konorov, S.O., Zheltikov, A.M., 2005. Photonic crystal fiber as a multifunctional optical sensor and sample collector. *Optics Express* 13, 3454–3459.
- Maulina, W., Rahmat, M., Rustami, E., Azis, M., Budiarti, D.R., Miftah, D.Y.N., Maniur, A., Tumanggor, A., Sukmawati, N., Alatas, H., Seminar, K.B., Yuwono, A.S., 2011. Fabrication and characterization of  $\text{NO}_2$  gas sensor based on one dimensional photonic crystal for measurement of air pollution index. *IEEE Proceedings of International Conference on Communication, Information, Instrumentation and Biomedical Engineering*, 352–355.
- Meixner, H., Gerblinger, J., Lampe, U., Fleischer, M., 1995. Thin-film gas sensors based on semiconducting metal oxides. *Sensor and Actuators B* 23, 119–125.
- Rahmat, M., Negara, T.P., Hardhienata, H., Irmansyah, Alatas, H., 2009. Real-time optical sensor based on one dimensional photonic crystals with defects. *IEEE Proceedings of International Conference on Communication, Information, Instrumentation and Biomedical Engineering*, 1–5.
- Sünner, T., Stichel, T., Kwon, S.-H., Schlereth, T.W., Höfling, S., 2008. Photonic crystal cavity based gas sensor. *Applied Physics Letters* 92 (261112).
- [USEPA] United States Environmental Protection Agency, 2006. 2002 National Emissions Inventory Booklet. North Carolina.
- Zhang, D., et al., 2004. Detection of  $\text{NO}_2$  down to ppb levels using individual and multiple  $\text{In}_2\text{O}_3$  nanowire devices. *Nanoletters* 4, 1919–1924.